Archives of Mechanics • Archiwum Mechaniki Stosowanej • 28, 5-6, pp. 1039-1055, Warszawa 1976

On the stability of the boundary layer along a concave wall

TH. HERBERT (FREIBURG)

VARIOUS approaches for investigating the linear stability of the laminar boundary layer along a concave wall with respect to Görtler vortices are compared concerning their order in the two small parameters, wall curvature and inverse Reynolds number, as well as the treatment of the curvature terms. Numerical results show separately the effects of wall curvature, streamline curvature and its finite extent on the neutral conditions. The influence of the growing boundary layer thickness on the stability characteristics is estimated and found to be of first order.

Porównano różne metody badania liniowej stateczności laminarnej warstwy przyściennej wzdłuż wklęsłej ściany (wirów Görtlera) ze względu na rząd dwóch małych parametrów: krzywizny ściany i odwrotności liczby Reynoldsa i uwzględniania członów z krzywizną. Wyniki liczbowe pokazują odpowiednio wpływ krzywizny ściany, krzywizny linii prądu i jej skończonego wydłużenia na warunki neutralne. Opracowano wpływ wzrostu grubości warstwy przyściennej na charakterystykę stateczności i wykazano, że jest pierwszego rzędu.

Сравнены разные подходы к исследованию линейной устойчивости ламинарного пограничного слоя вдоль вогнутой стенки (вихря Гертлера) из-за порядка двух малых параметров: кривизны стенки и обратной величины числа Рейнольдса и из-за учета членов с кривизной. Числовые результаты показывают соответственно влияние кривизны стенки, кривизны линии тока и ее конечного удлинения на неутральные условия. Обсуждено влияние роста толщины пограничного слоя на характеристику устойчивости и показано, что она первого порядка.

1. Introduction

THE OCCURRENCE of centrifugal instability in boundary layers along concave walls was first predicted theoretically by GÖRTLER [1] and is at present, well-established. The question of stability holds an important place not only within the context of heat exchange problems but also in studies of the transition region from laminar to turbulent boundary layer flow where experimental observations indicated vortex structures.

Obviously, an intensified appearance of the counterrotating longitudinal vortices cannot directly lead to turbulence, without a coupling with time-periodic disturbances, such as Tollmien-Schlichting waves or oblique waves. Experimental studies in the non-linear region show, indeed, meandering or pulsating vortices before breakdown sets in. Theoretical investigation of this coupling process would be an interesting application of the non-linear stability theory. It turns out, however, that the basis provided by the linear theory is rather incomplete and, partly, not sufficiently reliable.

Instability of the boundary layer flow along concave walls with respect to Tollmien-Schlichting waves has been studied by GÖRTLER [2]. He succeeded in extending the Rayleigh-Tollmien theorem to curved walls and found a slightly stabilizing influence of concave curvature. This seems to be the only investigation of time-periodic disturbances so that, up to now, even the neutral curve is unknown. Insofar as oblique waves are concerned, all attempts failed to extend Squire's theorem to the present configuration. TOLLMIEN and GROHNE [3] mention some unpublished work showing Squire's theorem not to be generally valid for concave walls. This result seems physically meaningful since a small deviation of the vortex axis from the streamwise direction should, by no means, change the stability limit in a radical way.

The usual assumption that curvature is of minor importance with regard to the properties of time-periodic disturbances is, therefore, not generally justified.

Considering the longitudinal vortices we find that the various theoretical investigations disagree as to the details of the formulation of the problem and as to their conclusions even on fundamental properties. For illustration let us take Fig. 1 which shows a survey of various neutral curves taken from the literature. All these curves are presumed to be the boundary between regions of stability and instability of the boundary layer flow with respect to Görtler vortices of wave number A, measured in terms of the Görtler number G. This survey is not at all complete. Some curves which resulted from inappropriate numerical treatment of the equations were left out.

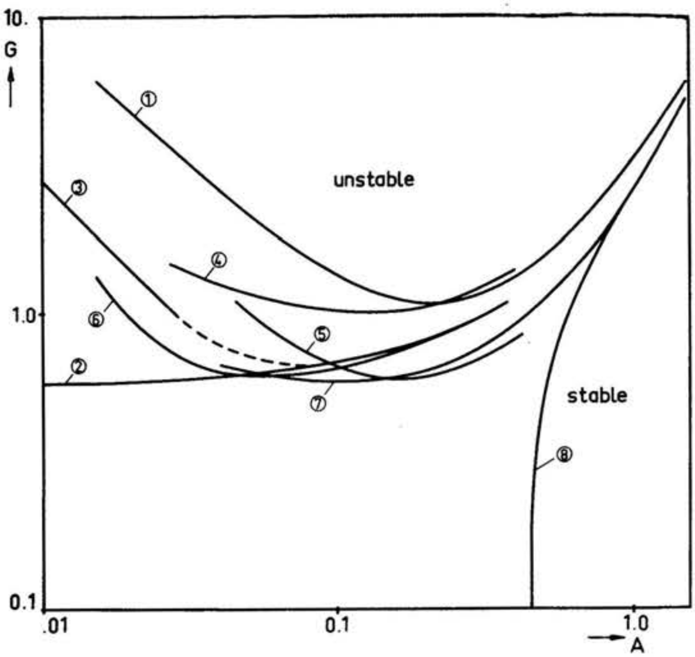

FIG. 1. Various neutral curves obtained with the parallel flow assumption.
(1) GÖRTLER [1], (2) HÄMMERLIN [9], (3) HÄMMERLIN [10], (4) HÄMMERLIN [12], (5) SCHULTZ-GRUNOW and BEHBAHANI [8], (6) KAHAWITA and MERONEY [14], and with the transverse velocity included (7) SMITH [11], (8) KAHAWITA and MERONEY [14].

It is inevitable that progress in analyzing vortex instability of boundary layers can only be achieved by using strong assumptions without a strict mathematical justification. Apart from the simplifications regarding the curvature of the flow, the assumptions mostly used were those successfully applied in treating the resistive wave instability of the flat-plate boundary layer. The latter is essentially connected with local properties of the basic velocity profile close to the critical layer. Vortex instability, however, is controlled by the more global balance of centrifugal forces with the other forces acting in the flow. Therefore, flow conditions outside the boundary layer must be carefully taken into account.

It is the aim of the following work to discuss various assumptions and to compare neutral curves resulting from different approximations by using a highly accurate numerical procedure. An improved analysis is suggested including the growing thickness of the boundary layer as well as the downstream variations of the vortex shape.

2. The governing equations

We shall consider the flow of a viscous incompressible fluid along a concave wall (Fig. 2). x represents the distance in the direction of the basic flow, measured along the wall from the leading edge, y ($\leqslant 0$) the distance normal to the wall and z the orthogonal coordinate in the spanwise direction. The velocity components in the directions x, y, z are u, v, w, respectively. $k = 1/r_0$ is the curvature of the wall, which is a continuous function $k = k(x)$ and is positive for concave walls. The equations governing the flow are the Navier-Stokes equations. In orthogonal curvilinear coordinates they are found ([4], where k is negative for concave walls) to be

$$\text{(2.1)} \quad \frac{\partial u}{\partial t}+\frac{1}{1-ky}u\frac{\partial u}{\partial x}+v\frac{\partial u}{\partial y}+w\frac{\partial u}{\partial z}-\frac{kuv}{1-ky}=-\frac{1}{\varrho(1-ky)}\frac{\partial p}{\partial x}$$
$$+\nu\left[\frac{1}{(1-ky)^2}\frac{\partial^2 u}{\partial x^2}+\frac{\partial^2 u}{\partial y^2}+\frac{\partial^2 u}{\partial z^2}-\frac{k}{1-ky}\frac{\partial u}{\partial y}-\frac{k^2u}{(1-ky)^2}-\frac{2k}{(1-ky)^2}\frac{\partial v}{\partial x}\right.$$
$$\left.+\frac{y}{(1-ky)^3}\frac{dk}{dx}\frac{\partial u}{\partial x}-\frac{1}{(1-ky)^3}\frac{dk}{dx}v\right],$$

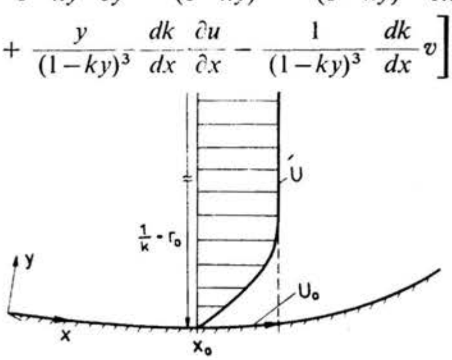

FIG. 2. Boundary layer flow along a concave wall.

and two similar equations in v and w. Here, p, ϱ and ν are respectively the pressure, density and kinematic viscosity. The continuity equation is

$$\text{(2.2)} \quad \frac{1}{1-ky}\frac{\partial u}{\partial x}+\frac{\partial v}{\partial y}-\frac{kv}{1-ky}+\frac{\partial w}{\partial z}=0.$$

In linear stability theory we consider, as usual, the flow as a superposition of a steady, two-dimensional basic flow and small disturbances in the form

$$\text{(2.3)} \quad \begin{aligned} u &= u_0(x,y)+u_1(x,y,z,t),\\ v &= v_0(x,y)+v_1(x,y,z,t),\\ w &= w_1(x,y,z,t),\\ p &= p_0(x,y)+p_1(x,y,z,t). \end{aligned}$$

Introducing Eq. (2.3) into Eqs. (2.1), (2.2) and linearizing in the disturbances yields two separate sets of equations respectively for the basic flow and the disturbances.

2.1. The basic flow

Even prior to the numerical analysis, the equations for the basic flow must be simplified by means of an order of magnitude analysis. The equations may be made non-dimensional by substituting

$$\begin{gathered} x = x_0 X = \mathrm{Re}\,\delta X, \quad y = \delta Y, \quad k = K/\delta, \\ u_0 = U_0 U, \quad v_0 = U_0 \bar{V} = U_0 V/\mathrm{Re}, \quad p_0 = \varrho U_0^2 P, \\ \delta = (\nu x_0/U_0)^{1/2}, \quad \mathrm{Re} = U_0 \delta/\nu, \quad \varepsilon = 1/\mathrm{Re}, \end{gathered} \tag{2.4}$$

where U_0 is the free stream velocity, x_0 the distance from the leading edge, δ the boundary layer thickness (*) and Re the Reynolds number. The relative magnitude of the terms may then be estimated in terms of the parameters ε and K which are both assumed to be small.

With $\varepsilon \ll 1$, $K \ll 1$, $dK/dX \leqslant 1$, and ε and K being of the same order of magnitude, the equations reduce to

$$\begin{gathered} \frac{1}{1-KY} U \frac{\partial U}{\partial X} + V \frac{\partial U}{\partial Y} + \frac{K}{1-KY} UV = -\frac{1}{1-KY}\frac{\partial P}{\partial X} + \frac{\partial^2 U}{\partial Y^2} \\ + \frac{K}{1-KY}\frac{\partial U}{\partial Y} - \left(\frac{K}{1-KY}\right)^2 U, \\ -\frac{K}{1-KY} U^2 = -\frac{\partial P}{\partial Y}, \\ \frac{1}{1-KY}\frac{\partial U}{\partial X} + \frac{\partial V}{\partial Y} - \frac{K}{1-KY} V = 0, \end{gathered} \tag{2.5}$$

where all the neglected terms are of the relative order ε^2 or less. A self-similar solution of these equations was found by MURPHY [5] and improved by SCHULTZ-GRUNOW and BREUER [6] for walls with $K = \text{const.}$, i.e., with the radius of curvature proportional to the boundary layer thickness.

In contrast to the foregoing, when $K \ll \varepsilon$, all the curvature terms are of the relative order ε^2 or less and thus can be neglected without changing the order of the approximation. Equations (2.5) then reduce to Prandtl's equations and the basic flow is represented by the Blasius' flow.

For $K \ll 1$, the solution of Eqs. (2.5) differs only slightly from Blasius' solution as far as boundary layer profile and momentum thickness are concerned. However, the potential flow outside the boundary layer introduced while solving Eqs. (2.5) is no longer a parallel flow. U tends to infinity as y approaches the center of curvature.

2.2. The disturbance equations

In order to simplify the disturbance equations, the conditions $\varepsilon \ll 1$, $K \ll 1$ and $dK/dX \leqslant 1$, which were already applied to the basic flow, can be introduced without deteriorating the approximation. However, it can not be anticipated that the disturbances

(*) The formal definition is chosen here since the physical boundary layer thicknesses may depend on curvature.

are limited to the boundary layer. The curvature terms which are negligible inside the boundary layer may well be important in the outer region.

Another aggravating aspect is the growing thickness of the boundary layer which, up to now, cannot be included in the analysis in a satisfactory manner (cf. Section 5). Since the transverse velocity $\bar{V}$ is small in comparison to U, the boundary layer flow is usually considered as a parallel flow, thus neglecting terms of order ε. A local stability analysis is then carried out using the Blasius' profile or the solution of Eqs. (2.5) at $x = x_0$ as the basic flow.

With the parallel-flow approximation the disturbances may be introduced in the form of longitudinal vortices which are independent of x and are amplified (or damped) in time

$$\begin{aligned} u_1 &= \hat{u}(y)\cos\alpha z e^{\beta t}, \\ v_1 &= \hat{v}(y)\cos\alpha z e^{\beta t}, \\ w_1 &= \hat{w}(y)\sin\alpha z e^{\beta t}, \\ p_1 &= \hat{p}(y)\cos\alpha z e^{\beta t}, \end{aligned} \tag{2.6}$$

where $\alpha = 2\pi/\lambda$ is the wave number, λ the wavelength and β the amplification rate.

After neglecting the small changes in curvature, dk/dx, the streamwise coordinate x is completely removed from the equations.

By substituting Eqs. (2.4) and

$$\begin{gathered} z = \delta Z, \quad \alpha = A/\delta, \quad \beta = B\nu/\delta^2, \\ \hat{u} = U_0 u, \quad \hat{v} = U_0\bar{v} = U_0 v/\mathrm{Re}, \quad \hat{w} = U_0 w, \quad \hat{p} = \varrho U_0^2 p \end{gathered} \tag{2.7}$$

the equations are made non-dimensional. Since no further use of the basic equations is needed, there should be no risk of confusion with the quantities defined in Eqs. (2.1), (2.2). The final set of disturbance equations is obtained after eliminating the pressure and the w-component of the velocity by using the continuity equation

$$\begin{aligned} &\frac{d^2u}{dY^2} - \frac{K}{1-KY}\frac{du}{dy} - \left[\tau^2 + \left(\frac{K}{1-KY}\right)^2\right]u = \mathrm{Re}\left[\frac{dU}{dY} - \frac{K}{1-KY}U\right]\bar{v}, \\ &\frac{d^4\bar{v}}{dY^4} - 2\frac{K}{1-KY}\frac{d^3\bar{v}}{dY^3} - \left[\sigma^2+\tau^2+3\left(\frac{K}{1-KY}\right)^2\right]\frac{d^2\bar{v}}{dY^2} \\ &\quad + \left[\sigma^2+\tau^2-3\left(\frac{K}{1-KY}\right)^2\right]\frac{K}{1-KY}\frac{d\bar{v}}{dy} + \left[\sigma^2\tau^2 + (\sigma^2+\tau^2)\left(\frac{K}{1-KY}\right)^2\right. \\ &\quad \left. -3\left(\frac{K}{1-KY}\right)^4\right]\bar{v} = -2\mathrm{Re}\sigma^2\frac{K}{1-KY}Uu, \end{aligned} \tag{2.8}$$

where $\tau^2 = A^2 + B$ and $\sigma = A$. Equations similar to Eqs. (2.8) were presented by BEHBAHANI and SCHULTZ-GRUNOW [7, 8], however, the right hand side of their second equation is erroneous.

The boundary conditions claiming that the disturbances must vanish at the wall can be restated by using the continuity equation as

$$u = v = \frac{dv}{dY} = 0 \quad \text{at} \quad Y = 0. \tag{2.9}$$

In the free stream the disturbances must decay. When using the boundary layer profile according to Eqs. (2.5) it follows

$$\frac{u}{U} = \frac{v}{U} = \frac{K}{1-KY}\frac{v}{U} - \frac{1}{U}\frac{dv}{dY} = 0 \quad \text{at} \quad Y = 1/K. \tag{2.10}$$

For the Blasius' profile ($U = 1$ at $Y = \infty$), these conditions reduce to the common form

$$u = v = \frac{dv}{dY} \quad \text{at} \quad Y = \infty. \tag{2.11}$$

2.3. Additional simplifications

In the set of disturbance equations originally presented by GÖRTLER [1], some additional simplifications were introduced in view of the smallness of K and because the disturbances were assumed to exist almost inside the boundary layer ($y \leqslant 5$). In detail he was led to the following assumptions:

(i) The curvature terms $(1-KY)^{-1}$ can be replaced by 1.

(ii) The terms multiplied by K can be neglected except those with the factor $\mathrm{Re}K$.

(iii) Inside the boundary layer, KU can be neglected in comparison with dU/dY.

With (i) – (iii) one obtains from Eqs. (2.8) the system

$$\begin{gathered} \frac{d^2u}{dY^2} - \tau^2 u = \frac{dU}{dY} v, \\ \frac{d^4v}{dY^4} - (\sigma^2+\tau^2)\frac{d^2v}{dY^2} + \sigma^2\alpha^2 v = -\mu\sigma^2 U u \end{gathered} \tag{2.12}$$

with the boundary conditions (2.9), (2.11), where $\mu = 2\mathrm{Re}^2K$. The Blasius' profiles represents the appropriate basic flow. The characteristic equation of this eigenvalue problem has the form

$$F(\sigma, \tau, \mu) = F(A, B, G) = 0, \tag{2.13}$$

thus providing an "universal" stability diagram. The parameters K and Re appear only implicit in the Görtler number

$$G = \left(\frac{\mu}{2}\right)^{1/2} = \mathrm{Re}K^{1/2}. \tag{2.14}$$

Görtler solved the eigenvalue problem by means of integral equations using Green functions. In accordance with his assumptions, the integrations were carried out only inside the boundary layer. His result was the now well-known stability diagram, predicting the onset of instability at $G \simeq 1$, and a wave number $A \simeq 0.2$. The neutral curve ($B = 0$, i.e., $\tau = \sigma$) is shown in Fig. 1.

HÄMMERLIN [9] resolved Eqs. (2.12); his improved analysis provided a minimum of the neutral curve at $A = 0$ where the vortices (2.6) disappear. At the same time he found the vortices at small A to reach far beyond the edge of the boundary layer and thus Görtler's assumptions not to be valid for all wave numbers. Consequently, in [10] he dropped the assumption (iii) and obtained the equations

$$\frac{d^2u}{dY^2}-\tau^2u=\left[\frac{dU}{dY}-KU\right]v,$$
(2.15)
$$\frac{d^4v}{dY^4}-(\sigma^2+\tau^2)\frac{d^2v}{dY^2}+\sigma^2\tau^2v=-\mu\sigma^2Uu$$

instead of Eq. (2.12). The related characteristic equation is now

(2.16) $$F(\sigma,\tau,\mu,K)=F(A,B,G,K)=0,$$

and the stability diagram depends explicitly on K. The equations (2.12) turn out to be the limit for $K\to 0$.

Apart from some asymptotic properties obtained for a simplified linear boundary layer profile, Eqs. (2.15) have never been solved numerically.

2.4. Treatment of streamline curvature

The crucial difference between the approximations (2.8) and (2.15) lies in the treatment of the curvature terms. Since the centrifugal forces drive the secondary vortex flow, it is obvious that the wall curvature K itself plays a less important role than the overall curvature of the flow field.

Equations (2.8) are based on a curvature of the streamlines tending to infinity like $(1-KY)^{-1}$ as it is shown in Fig. 3a. All the terms multiplied by powers of $K/(1-KY)$, must be retained in this case since they receive importance close to the singularity. Therefore the equations may be regarded as exact in some sense. However, the assumption of an infinite streamwise extent of the wall having a constant curvature K gives rise to some questions, especially in view of the local character of the theory. In practice, wall curvature is present only over a certain part of the wall and no singularity appears. Therefore, it seems justified to introduce more realistic properties of the flow far from the wall.

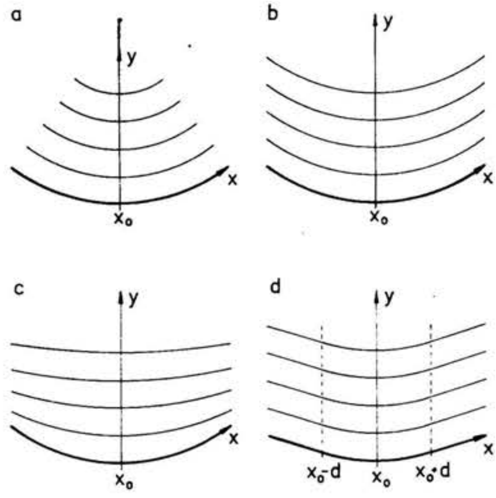

FIG. 3. Various models for wall curvature and streamline curvature.

The assumption (i) applied in Eqs. (2.12) and (2.15) implies the streamline curvature to be constant at any distance from the wall, as it is shown in Fig. 3b.

Another model has been introduced by SMITH [11]. The terms $(1-KY)^{-n}$ are replaced by their series expansion and only the first terms $(1+nKY)$ are retained. Thus, the singularity at $KY = 1$ is removed to $Y = \infty$. In a similar way one could replace $(1-KY)$ by other functions, for example by $\exp(KY)$.

Such approximations are in effect equivalent to changes of the outer flow conditions and should already be taken into account while deriving the equations. This idea has been followed by HÄMMERLIN [12] using locally an outer flow which has the properties of the boundary layer flow along a wavy wall in the valley positions. There, streamline curvature decays like $K\exp(-CY)$ (Fig. 3c). The streamlines are utilized to construct a net of locally-orthogonal curvilinear coordinates. Starting from transformed basic equations, for disturbances of the form (2.6) and sufficiently small wall curvature the following disturbance equations are obtained:

$$\frac{d^2u}{dY^2}-\tau^2u=\frac{dU}{dY}v,$$

(2.17)

$$\frac{d^4v}{dY^4}-(\sigma^2+\tau^2)\frac{d^2v}{dY^2}+\sigma^2\tau^2v=-\mu\sigma^2Ue^{-CY}.$$

In this approximation the decay of the streamline curvature affects only the right hand side of the second equation. The additional term introduced in the first Eq. (2.15) has been dropped here since in the new coordinates $dU/dY-KU$ vanishes in the potential flow. This condition, however, is not satisfied by the Blasius' profile which has been applied in HÄMMERLIN'S [12] analysis. For $C = 0$, the Eqs. (2.17) as well as the outer flow reduce exactly to Görtler's formulation (2.12)

Finally, an analysis has been carried out by TOBAK [13] for a wall having concave curvature only over a finite streamwise extent (described by the parameter $d = \delta D$ in Fig. 3d) and being plane elsewhere. Eliminating the variable X by means of Fourier transforms and introducing Görtler's assumptions (i)–(iii), the following set of equations is obtained:

$$\frac{d^2u}{dY^2}-\tau^2u=\frac{dU}{dY}v,$$

(2.18)

$$\frac{d^4v}{dY^4}-(\sigma^2+\tau^2)\frac{d^2v}{dY^2}+\sigma^2\tau^2v=-\mu\sigma^2Uu(1-e^{-AD}).$$

The finite extent of the curvature appears only as a multiplier to the Görtler number. Thus, after having solved Eqs. (2.12) with Eqs. (2.9), (2.11), the eigenvalues of Eqs. (2.18) can be obtained by a simple transformation without repeating the numerical analysis. The stability diagrams presented in [13] are derived from the results in [1] which were already subject to criticism.

In spite of the shortcomings involved in the various approximations, a numerical evaluation of the equations (2.15), (2.17) and (2.18) seems valuable. It turns out that these equations are appropriate for studying separately the influences of wall curvature, decay of streamline curvature and finite extent of wall curvature on vortex instability. Improved results of the disturbance equations (2.8) will be presented using the boundary layer profile (2.5) for curved walls. In addition, Eqs. (2.12) will be solved since they provide the limiting values of all the other approximations.

3. Method of solution

Various methods are used to obtain numerically the solutions, i.e., eigenvalues and eigenfunctions of the disturbance equations. GÖRTLER [1] and HÄMMERLIN [9] first transformed the differential equations to a system of integral equations which were solved numerically when the integrals were replaced by finite sums. SMITH [11] and others used Galerkin's method to calculate the eigenvalues. The resulting eigenfunctions, however, are subject to some criticism. The more recent investigations apply difference methods, such as the Runge-Kutta method, for the numerical integration of the equations within the boundary layer which are matched at the boundary layer edge to an outer analytical solution. The outer solution is constructed in the form of a fundamental system from the disturbance equations which are simplified after replacing U by the outer potential flow. According to the outer boundary conditions, only three of the initially six fundamental solutions have to be taken into account.

Usually, inside the boundary the disturbance equations are treated as an initial value problem starting from the wall. Matching the numerical results at a position $Y = Y_m$ sufficiently far outside the boundary layer with a linear combination of the three fundamental solutions provides the eigenvalue relation. In the present investigation the integration is, as in [14], carried out in the reverse direction, starting from Y_m to the wall. The boundary conditions at the wall are satisfied by iterative improvement of an initially guessed eigenvalue. The highly accurate difference scheme combined with conditional filtering which was applied here has already been successfully used in the numerical treatment of non-linear stability problems for the flat plate [15]. Since the parasitic fundamental solutions decay in the direction to the wall, the numerical stability of the procedure is improved; this makes the method more accurate and efficient.

All the results presented in this paper were obtained with a stepsize of 0.125 starting at $Y_m = 10$. The calculations were carried out on the UNIVAC 1106 of the University Freiburg.

3.1. The outer solutions

For sufficiently large Y_m the Blasius' profile satisfies approximately

$$U \equiv 1, \quad \frac{dU}{dY} \equiv 0 \quad \text{for} \quad Y \geqslant Y_m. \tag{3.1}$$

Introducing this into the disturbance equations (2.12), (2.15), (2.17), (2.18) and eliminating u, one can easily find the related fundamental system for v in the form $v_i = Y^p \exp(\varrho_i Y)$, $i = 1, \ldots, 6$, where ϱ_i are the roots of the characteristic equations and $p > 0$ appears in the case of multiple roots. The u_i can afterwards be derived from v_i using the second disturbance equation. For the parameters of interest, only three roots with negative real parts are obtained. The related solutions u_i, v_i satisfy the outer boundary conditions (2.11) and are continued from Y_m to the wall by numerical integration.

With regard to the disturbance equations (2.8) based on the improved boundary layer profile according to Eqs. (2.5), we consider here only the case of neutral disturbances $(B = 0)$. Introducing the outer flow

$$U = U_0/(1-KY), \tag{3.2}$$

$v = \mathrm{Re}\bar{v}$ and the transformation

$$\eta = (1-KY)A/K \tag{3.3}$$

the equations reduce to

$$\eta^2 \frac{d^2u}{d\eta^2} + \eta \frac{du}{d\eta} - (1+\eta^2)u = 0,$$

$$\eta^4 \frac{d^4v}{d\eta^4} + 2\eta^3 \frac{d^3v}{d\eta^3} - (3+2\eta^2)\frac{d^2v}{d\eta^2} + (3-2\eta^2)\eta\frac{dv}{d\eta} - (3-2\eta^2-\eta^4)v = -\frac{\mu}{K^2}\eta^2 u. \tag{3.4}$$

Apart from a mistake in the right hand side of the second equation, similar equations were already presented in [7, 8]. Obviously, the first equation is seen to be the modified Bessel operator with the solutions

$$u_1 = \eta I_1(\eta), \quad u_4 = \eta K_1(\eta), \tag{3.5}$$

where only u_1 satisfies the boundary condition (2.10). The fundamental solutions v_i are given in [7, 8] as power series in η.

On the other hand, analytical solutions of the homogeneous second equation can be found in the form

$$v_2 = I_1(\eta), \quad v_3 = \eta I_0(\eta), \quad v_5 = K_1(\eta), \quad v_6 = \eta K_0(\eta) \tag{3.6}$$

and as a particular solution constructed from u_1 one first obtains

$$\tilde{v}_1 = c\left[\frac{1}{\eta} I_0(\eta) - \ln\eta I_1(\eta)\right], \quad c = -\frac{4K^2}{\mu}. \tag{3.7}$$

So far, only v_2 and v_3 satisfy Eq. (2.10). The singular behaviour of $\tilde{v}_1$ at $\eta = 0$, however, can be removed through combination with v_5, v_6, resulting in

$$v_1 = c\left[\frac{1}{\eta} I_0(\eta) - \ln\eta I_1(\eta) - K_1(\eta) - \eta K_0(\eta)\right]. \tag{3.8}$$

The three fundamental solutions to be continued to the wall are finally (u_1, v_1), $(0, v_2)$, $(0, v_3)$.

The advantage of using the analytical form of the outer solution is obvious since large values of η may arise from the small curvature K. Series expansions of the Bessel functions are useless for numerical evaluation in that case. The series provide numerical data with the required accuracy only in the case of large curvature (which contradicts the assumption of the theory), very small wave numbers (which may be of minor interest) or Y_m close to the singularity at $Y = 1/K$ (thus increasing drastically the computational effort). The analytical form, on the contrary, simply allows the use of the asymptotic properties of the functions. However, even then care must be taken in order to maintain linear independence in the numerical representation of the fundamental solutions and their derivatives at Y_m.

4. Results and discussion

Although the computer program is written to calculate eigenvalues and eigenfunctions according to the various approximations for any parameters of practical interest, only neutral curves are presented here. In addition, the investigations are limited to the classical and most unstable mode. Higher modes, which may well be of physical importance, are discussed in [16].

The results of Hämmerlin's equations (2.15), (2.9), (2.11) are shown in Fig. 4 and compared with the limiting curve obtained from Görtler's equations (2.12). Apart from some slight differences caused by the underlying basic flow and the numerical method, the lowest curve agrees well with HÄMMERLIN's result [9]. As to Eqs. (2.15), up to now only the asymptotic property $G \sim K^{1/4}A^{-1}$ of the neutral curves for small A and for a simple linear appro-

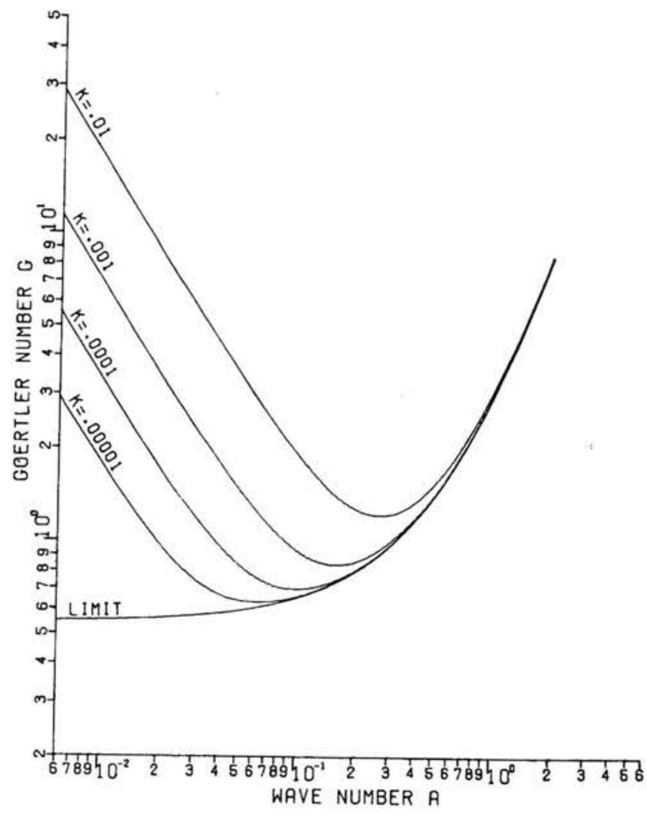

FIG. 4. Neutral curves for various values of the wall curvature K (Eqs. (2.15)).

ximation to the boundary layer profile were given in [10]. With $K = \text{const.}$, the relation $G \sim A^{-1}$ is confirmed by the numerical results for the Blasius' profile too but the constant of proportionality depends on K in a more complicated way.

The critical conditions (marked with an index c) derived from the minima of the neutral curves vary with curvature K and are shown in Fig. 5. There is a considerable change in the wave number A_c, which is related to the selective occurrence of a preferred wave length in experiments. The critical value Λ_c of the wave-length parameter $\Lambda = (\lambda/\delta)^{3/2} G$ is also drawn in Fig. 5. The critical Görtler number G_c is slightly increased by increasing K. At the same time, the critical Reynolds number derived from Eq. (2.14) decreases to very low values, e.g., $\text{Re}_c = 12.2$ at $K = 0.01$. Since the transverse velocity terms (of order $\varepsilon = \text{Re}^{-1}$) are neglected, only very small curvature is within the scope of the theory.

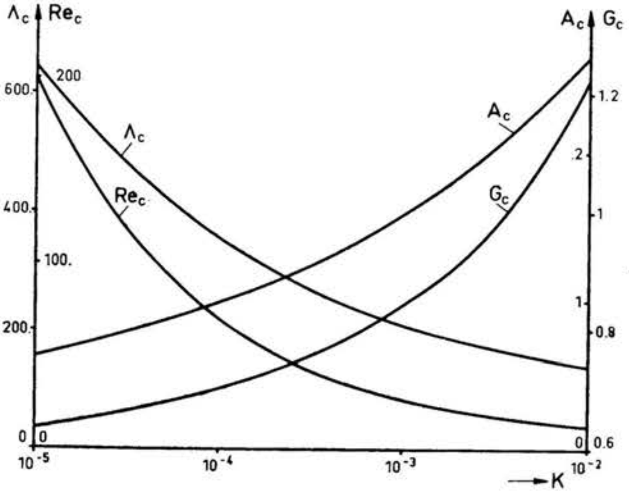

FIG. 5. Critical values of the wave number A_c, Görtler number G_c, Reynolds number Re_c and wavelengt parameter Λ_c versus wall curvature K (Eqs. (2.15)).

Equations (2.17) were numerically treated by HÄMMERLIN's [12] only for the fixed value $C \approx 0.1$. As it is shown in Fig. 6, by variation of C, i.e., the decrease of streamline curvature far from the wall, one can produce a stability diagram similar to that given in Fig. 4 without changing K. The wall curvature K appears only implicitly in $G = \text{Re}\, K^{1/2}$, thus the critical Reynolds number increases here with increasing G_c. The stabilizing effect of an increase in C can be explained by the smaller extent of the curved flow region (in y) and the related reduction of the driving centrifugal forces in the outer flow.

A similar situation can be found on the basis of Tobak's equations (2.18). The results shown in Fig. 7 were obtained by transforming the data resulting from Eqs. (2.12). Even here, diminishing the (streamwise) extent of the curved flow region causes an increase of the critical Görtler number and Reynolds number.

Since each of the approximations (2.15), (2.17) and (2.18) just excludes the influences introduced in the other two, Figs. 4, 6 and 7 show the three separate mechanisms producing independently about the same quantitative influence on the neutral curve in terms of the Görtler number. This is of particular interest while comparing theoretical and experimental

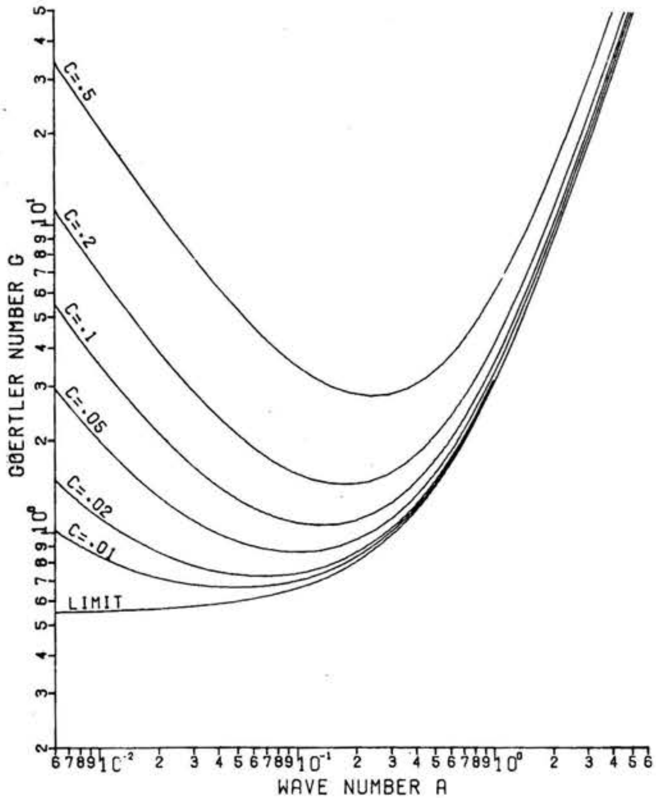

FIG. 6. Neutral curves depending on the decrease exp($-CY$) of the streamline curvature (Eqs. (2.17)).

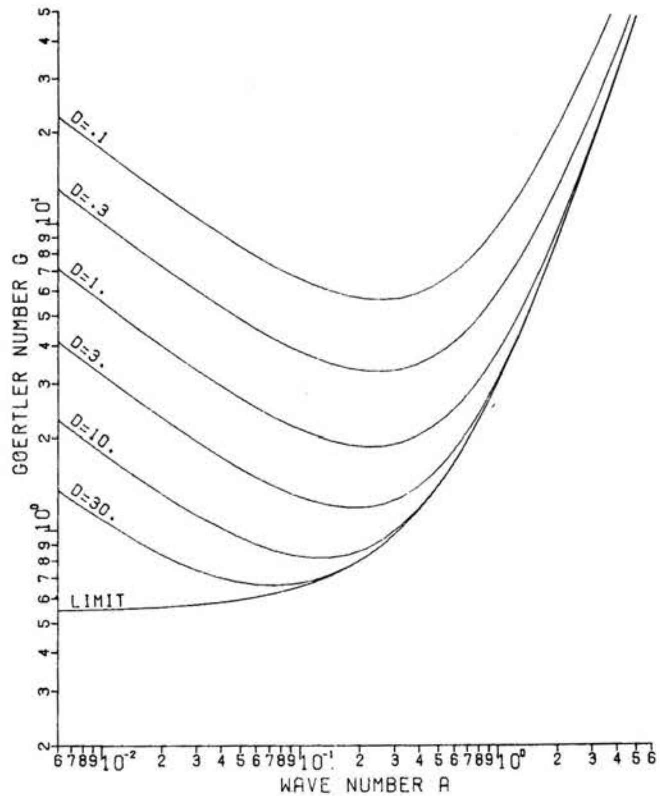

FIG. 7. Neutral curves depending on the streamwise extent D of the wall curvature (Eqs. (2.18)).

amplification rates. Apart from the difficulties in identifying neutral conditions with sufficiently small disturbances, an experimental verification of the theory requires a detailed specification of the underlying flow conditions, especially in the low (and critical) wave number region. The ascending branch at larger wave numbers does not change considerably, therefore BIPPES' comparison with experimental data [17] may be regarded as conclusive.

The difference between the theoretical and experimental results concerning neutral stability cannot be removed by using the approximation suggested by SCHULTZ-GRUNOW and BEHBAHANI [8]. Figure 8 shows the results obtained from Eqs. (2.8)–(2.10). Since curvature of the streamlines increases with increasing distance from the wall, the neutral curves run below the limiting curve according to Eqs. (2.12) in a wide range of wave numbers, and finally rise with decreasing A. This sudden rise and consequently, the critical wave number is strongly connected with the modified Bessel functions of second kind in the outer solution which comes into play at the edge of the boundary layer. This occurs at a fixed value of η and, therefore, A_c should be approximately proportional to K. As can be seen in Fig. 8, the calculations provide the estimate $A_c \approx 3.5K$, which may be extremely small when compared to the values shown in Fig. 5. Even G_c and Re_c are smaller here due to the intensified centrifugal forces.

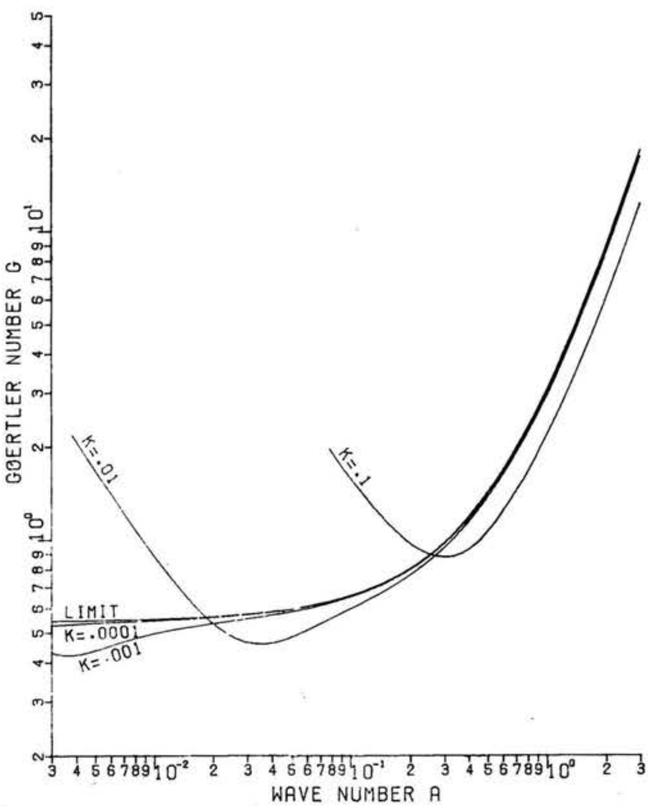

FIG. 8. Neutral curves for various values of the wall curvature K (Eqs. (2.8)).

The neutral curves in Fig. 8 disagree essentially from those presented by SCHULTZ-GRUNOW and BEHBAHANI [7, 8, 18]. Unfortunately, some mistakes in the notations used in their papers make it difficult to explain the discrepancy fully. Probably the results suffer from the fact that the series representation of the outer solution are used without the required care.(1)

Apart from this, the large values chosen for the wall curvature K might well be outside the scope of the theory, for they result in extremely small critical Reynolds numbers $\mathrm{Re}_c < 10$, where the disturbance equations as well as the boundary layer theory fail to provide a valid solution. At the onset of vortex instability, typical Görtler numbers are about $G = \mathrm{Re}\,K^{1/2} \approx 1$. Thus, we find $K \approx \mathrm{Re}^{-2}$ and the largest terms (of order $\mathrm{Re}\,K \approx \approx \mathrm{Re}^{-1}$) introduced by the curvature to be comparable in magnitude with the neglected transverse velocity terms. It follows that an extension and improvement of the theory presented by HÄMMERLIN [10] first requires the involvement of higher order terms in Re^{-1}, not K. At the same time the influence of the growing thickness of the boundary layer on vortex instability must be expected to be of first order.

5. The effect of the growing thickness

All the approximations mentioned so far suffer from the assumption of the boundary layer to be locally a parallel flow. A first attempt to improve this situation has been made by SMITH [11] taking into account the transverse velocity in the boundary layer. Small streamwise changes in curvature were found to be of minor importance. In contrast to Eqs. (2.6), the vortices are assumed to grow with distance x, not time:

$$
\begin{aligned}
u_1 &= \hat{u}(y)\cos\alpha z e^{\beta x},\\
v_1 &= \hat{v}(y)\cos\alpha z e^{\beta x},\\
w_1 &= \hat{w}(y)\sin\alpha z e^{\beta x},\\
p_1 &= \hat{p}(y)\cos\alpha z e^{\beta x}.
\end{aligned}
\tag{5.1}
$$

Starting from Eqs. (2.1)–(2.3), the usual procedure leads to a set of equations which were further simplified replacing $(1-KY)^{-n}$ by its series expansion $(1+nKY+\ \ldots)$ and linearizing in the small parameter K. For neutral disturbances the resulting equations are

$$
\begin{aligned}
&\frac{d^2u}{dY^2}-(V+K)\frac{du}{dy}-\left(\sigma^2-\frac{dV}{dY}\right)u = \left(\frac{dU}{dY}-KU\right)v,\\
&\frac{d^4v}{dY^4}-(V+2K)\frac{d^3v}{dY^3}-\left(2\sigma^3+\frac{dV}{dY}-KV\right)\frac{d^2v}{dY^2}+\left(\sigma^2V+2K\sigma^2+K\frac{dV}{dY}\right)\frac{dv}{dY}\\
&\qquad\qquad+\sigma^2\left(\sigma^2+\frac{dV}{dY}\right)v = -\mu\sigma^2Uu.
\end{aligned}
\tag{5.2}
$$

Since $V = \mathrm{Re}\,\bar{V}$ is of the same magnitude as U, the terms introduced by the growing thickness cannot be regarded as small. It must be expected that the transverse velocity is of considerable importance for vortex instability, especially in the low wave number region ($\sigma =$

(1) Corrected results have been published in a Brief Report by D. BEHBAHANI, ZAMP, **26**, 493–495, 1975.

$= A < 1$). It is the lack of such terms, introduced by the boundary-layer growth, which accounts for the parallel-flow equations to fail for $K = 0$, where decaying vortices are expected to exist, and for their inadequacy in describing forced vortices as they are produced by non-linear interaction of three-dimensional disturbances [15].

In spite of these qualitative conclusions, the numerical results presented by SMITH differ only moderately from those obtained with the parallel-flow assumption, (Fig. 1). However, the calculations carried out by KAHAWITA and MERONEY [14] on the basis of Smith's equations with and without inclusion of the transverse flow terms (Fig. 1, curves (6) and (8) respectively) show a remarkable difference. With the V-terms included, no critical value is obtained for G and the neutral curve seems to reach a limiting wave number of about $A \approx 0.45$ at $G = 0$. In tendency, this change in the stability characteristic agrees well with the results of HAALAND and SPARROW [19] for vortex instability of natural convection, where the accounting of the non-parallel nature of the basic flow has a first order effect.

The reason for the discrepancy between Smith's result and that of Kahawita and Meroney can not be completely explained up to now. Some preliminary investigations in this aspect tend to confirm the latter results.

Kahawita and Meroney already suspected the physically strange stability characteristic to be due to an inaccurate mathematical description of the physical situation. Indeed, this is true, for in a growing boundary layer the amplification rate and, moreover, the shape of the vortices will depend on the streamwise distance x. An order of magnitude analysis shows the terms introduced by these streamwise changes of vortex shape to be of the same order as the transverse velocity terms.

In the treatment of Tollmien-Schlichting waves, where the growing thickness turns out to be less important, some success has been reached by using perturbation methods (cf. [20]). In the present case, however, the difficulties in deriving a set of appropriate and accessible equations are not yet completely overcome.

References

1. H. GÖRTLER, *Über eine dreidimensionale Instabilität laminarer Grenzschichten an konkaven Wänden*, Nachr. Wiss. Ges. Göttingen Math.-Phys. Kl., 1–26, 1940.
2. H. GÖRTLER, *Über den Einfluß der Wandkrümmung auf die Entstehung der Turbulenz*, ZAMM, **20**, 138–147, 1940.
3. W. TOLLMIEN, D. GROHNE, *The nature of transition, Boundary layer and flow control*, Pergamon Press, Oxford, London, New York, Paris, 602–636, 1961.
4. S. GOLDSTEIN, *Modern developments in fluid dynamics*, Clarendon Press, Oxford 1938.
5. J. S. MURPHY, *Some effects of surface curvature on laminar boundary layer flow*, J. Aero, Sci., **20**, 338–344, 1953.
6. F. SCHULTZ-GRUNOW, W. BREUER, *Laminar boundary layers on cambered walls, Basic developments in fluid dynamics* (ed. M. Holt), Academic Press, New York and London, Vol. 1, 377-436, 1965.
7. D. BEHBAHANI, *Dreidimensionale Grenzschicht-Instabilität*, Dissertation Aachen 1971.
8. F. SCHULTZ-GRUNOW, D. BEHBAHANI, *Boundary layer stability at longitudinally curved walls*, ZAMP, **24**, 499–506, 1973.
9. G. HÄMMERLIN, *Über das Eigenwertproblem der dreidimensionalen Instabilität laminarer Grenzschichten*, J. Rat. Mech. Anal. **4**, 279–321, 1955.

10. G. HÄMMERLIN, *Zur Theorie der dreidimensionalen Instabilität laminarer Grenzschichten*, ZAMP **7**, 156-164, 1956.
11. A. M. O. SMITH, *On the growth of Taylor-Görtler vortices along highly concave walls*, Quart. Appl. Math., **13**, 233-262, 1955.
12. G. HÄMMERLIN, *Über die Stabilität einer kompressiblen Strömung längs einer konkaven Wand bei verschiedenen Wandtemperaturverhältnissen*, Deutsche Versuchsanstalt für Luftfahrt, Bericht 176, 1961.
13. M. TOBAK, *On local Görtler instability*, ZAMP, **22**, 130-143, 1971.
14. R. A. KAHAWITA, R. N. MERONEY, *The stability of parallel, quasi-parallel and stationary flows*, Project Themis TR 24, Colorado State University, Fort Collins, 1973.
15. Th. HERBERT, *Über endliche Amplituden periodischer Störungen der Grenzschicht and der ebenen Platte*, Deutsche Luft- und Raumfahrt, Forschungsbericht, 74-53, 1974.
16. Th. HERBERT, *Höhere Eigenzustände der dreidimensionalen Instabilität laminarer Grenzschichten* [to be published].
17. H. BIPPES, *Experimentelle Untersuchung des laminar-turbulenten Umschlags an einer parallel angeströmten konkaven Wand*, Dissertation, TU Berlin 1972.
18. F. SCHULTZ-GRUNOW, D. BEHBAHANI, *Dreidimensionale Grenzschicht-Instabilität*, ZAMM, **52**, T113-T114, 1972.
19. S. E. HAALAND, E. M. SPARROW, *Vortex instability of natural convection flow on inclined surfaces*, Int. J. Heat Mass Transfer, **16**, 2355-2367, 1973.
20. M. GASTER, *On the effects of boundary-layer growth on flow stability*, J. Fluid Mech. **66**, 465-480, 1974.

INSTITUT FÜR ANGEWANDTE MATHEMATIK
DER ALBERT-LUDWIGS-UNIVERSITAT.

Received February 27, 1976.